IEEE Access
Multidisciplinary | Rapid Review | Open Access Journal

Received January 28, 2020, accepted February 14, 2020, date of publication March 2, 2020, date of current version March 19, 2020.

Digital Object Identifier 10.1109/ACCESS.2020.2977663

Multi-Level DC/DC Converter for E-Mobility Charging Stations

SANG-KIL LIM[1], (Member, IEEE), HAE-SOL LEE[2,3], (Student Member, IEEE), HYUN-ROK CHA[2], AND SUNG-JUN PARK[4], (Member, IEEE)

[1]Department of Automotive Engineering, Honam University, Gwangju 62399, South Korea
[2]Korea Institute of Industrial Technology, EV Components and Materials R&D Group, Gwangju 61012, South Korea
[3]Department of Robotics, University of Science and Technology, Daejeon 34113, South Korea
[4]Department of Electrical Engineering, Chonnam National University, Gwangju 61186, South Korea

Corresponding author: Sung-Jun Park (sjpark1@jnu.ac.kr)

This work was supported by the Korea Institute of Industrial Technology [Manufacture and develop E-PTO and charge/discharge system of electric UTV and electric tractor (1/1)] under Grant KITECH IR-18-0680.

ABSTRACT The interest in electric-powered transportation has been increased because of problems such as depletion of fossil fuel resources and environmental issues caused by internal combustion engines. The market for various kinds of small E-mobility devices (EMDs), such as electric vehicles (EVs), E-bikes, segways, and mini-boards has been growing rapidly. Of these, the distribution of the small electric vehicles called personal mobility devices (PMDs), which can address problems such as traffic issues and environmental pollution, is expected to gain momentum. However, unlike the widely used charging stations for EVs, charging systems for PMDs are insufficient. The large size of dedicated PMD charging adapters makes them inconvenient to transport. Therefore, to make PMDs more attractive, it is necessary to deploy charging stations that can charge all types of PMDs. The present study proposes a new charging system that can respond to the needs of PMDs having various voltages and implement low charging current ripple. The proposed multi-level charging system can share power by subdividing the power supply to handle the charging requirements of various PMDs. In order to verify the validity of the proposed charging system, we performed simulations and conducted experiments by building a prototype charging system.

INDEX TERMS Electric vehicles (EVs), dc/dc converter, personal mobility devices (PMDs), multi-level charging system, E-mobility.

I. INTRODUCTION

Recently, because of problems such as depletion of fossil fuel resources and environmental issues, the conventional approach to transportation power has been shifting from internal combustion engines to electricity [1]–[3]. In particular, energy agencies around the world, including the U.S. Department of Energy are promoting a technology roadmap for eco-friendly transportation using electricity as a power source that can compete with traditional fossil fuel vehicles. Therefore, the market for various kinds of E-mobility devices, such as electric vehicles, E-bikes, and electric kickboards has been rapidly growing as an eco-friendly means of transportation. ''E-Mobility'' refers to electric-drive vehicles that use electricity as the main power source and need a charger or charging infrastructure to charge the device's batteries. E-mobility includes personal mobility devices (PMDs), smart mobility devices (SMDs), and micro mobility devices (MMD), as are illustrated in Figure 1. In particular, among E-mobility devices, the demand for PMDs as a means of personal transportation for one or two people is sharply increased [4], [5].

The reasons for the demands can be largely divided into environmental and social aspects. First, from an environmental aspect, it can be a means of reducing environmental pollution caused by traffic jams and congestion in metropolises around the world [6]. Second, from a social aspect, it can serve the needs of the growth of one- and two-person households and the changing perception of transportation from ownership to use. Because of these and other factors, even automobile manufacturers and automobile parts manufacturers are now entering the PMD market, which is likely to

The associate editor coordinating the review of this manuscript and approving it for publication was Narsa T. Reddy.

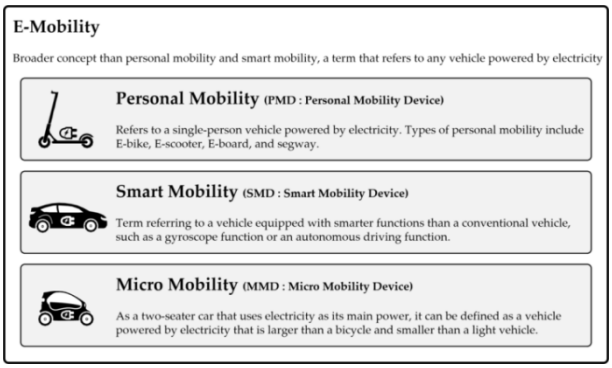

FIGURE 1. E-Mobility classification.

accelerate the distribution and commercialization of PMDs, such as electric bicycles that are effective for short distance.

In the case of E-mobility devices such as electric vehicles, whose distribution is widespread, charging is easy because charging stations are well established. However, charging stations for the newly and sharply growing market for small- and medium-sized E-mobility devices are so insufficient that they are instead charged by personal charging devices.

E-mobility charging systems, compact external adapters operating in a commercial power supply (220VAC) environment, must be designed to satisfy electrical appliance certification standards, such as electromagnetic interference (EMI) regulations, Power Factor Correction (PFC) regulations, and safety standards [7]–[9]. However, because of these requirements, it is inconvenient to carry such devices because of their volume and weight. Therefore, there is a need for the development of a charging system suitable for charging stations that can charge E-mobility devices such as scooters or electric bicycles with small- and medium-sized power requirements.

The requirements for a charging system suitable for charging stations can be summarized into the following two main factors: First, the output voltage control region of the charging system must be wide in order to charge equipment with a wide variety of voltages ranging from 12V to 60 V, depending on the device manufacturer and equipment characteristics.

Second, the current ripple rate required by batteries in all chargeable regions must be satisfied in order to charge various types of E-mobility equipment with a single charging system. Therefore, in order to satisfy the ripple rate of the charging current, regardless of the charging current required in all chargeable voltage regions ranging from 12 V to 60 V, there is a need for a new charging topology and a switching technique that can operate it.

The present paper proposes a new multi-level charging topology and a switching technique that can be applied in a wide range of charging voltages and produce low charging current ripple. The multi-level charging system proposed in this paper is designed to reduce the production cost of the system by using a low cost AC / DC converter through mass production. The proposed multi-level charging system can supply power by subdividing the power supply to handle the charging requirements of various types of E-mobility equipment. Therefore, the proposed charging system has the advantage of reducing the Total Harmonic Distortion (THD) sensitivity of the input current according to the output voltage and power, unlike traditional charging systems where the THD of the input current changes sharply according to the output voltage. In order to verify the validity of the proposed charging system, we performed simulations using PSIM and conducted experiments by building a 1200-W charging system.

The remainder of this paper is organized as follows: Section 2 describes the background of the personal mobility device market. Hardware descriptions of the multi-level charging system are presented in Section 3. Then, Section 4 discusses the battery charging simulation results and the experiment with operation of the multi-level converter. Finally, our conclusions are presented in Section 6.

II. BACKGROUND: PERSONAL MOBILITY DEVICE MARKET

The PMD market started in 2001 with the introduction of the Segway personal vehicle. Currently, various types of products, such as single-wheel and two-wheel Segway vehicles and electric bicycles are produced and sold by various companies including global automobile brands to auto parts manufacturers. Although it is difficult to define the PMDs form unambiguously, PMDs has the common features of being eco-friendly, portable, and easy to move a short to medium distance using electricity as a power source. Table 1 summarizes various types of PMDs currently on the market [10]–[12].

As shown in Table 1, PMDs commonly employ a charging method using a dedicated charger with an External Adapter (EA) regardless of shape and type, but the voltage range of the batteries varies depending on the manufacturer and PMD type. Therefore, a dedicated PMD adapter should be prepared at all times that guarantees only a short to medium distance in case the battery runs down while moving. However, because chargers with external adapters use a commercial power supply of 220 VAC, they must be implemented to satisfy the certification standards of electrical appliances,

TABLE 1. Types of personal mobility on the market.

Manufacture	Kinds	Battery	Operation Voltage	Charging Type
Cross	E-bike	Li-ion	36V	OFBC
Unibike	E-bike	Li-ion	36V	OFBC
Ecobike	E-bike	$LiFePO_4$	36V	OFBC
Hyundai	E-scooter	Li-ion	36V	OFBC
Coclever	E-scooter	Li-ion	36V	OFBC
Yuneec	E-board	Li-ion	24V	OFBC
Segway	1 wheel Segway	Li-ion	63V	OFBC
Segway	E-wheel	Li-ion	24V	OFBC
Razor	E-heel wheel	Li-ion	12V	OFBC

*OFBC: Off–Board Charger

which leads to an increase in the volume and weight, thus making them inconvenient to carry. Therefore, there is a need for charging stations that can charge PMDs away from home; however, it is not easy to deploy charging stations because the battery voltage range of each manufacturer is different [13], [14]. Therefore, for the widespread use of PMDs as a means to address traffic issues and environmental pollution, there is a need for charging stations capable of charging all types of PMDs. The requirements of charging stations for charging PMDs must satisfy safety standards including the current ripple rate required by batteries with a wide range of charging voltage [15].

III. MULTI-LEVEL CHARGING SYSTEM FOR PMDs

A. HARDWARE DESCRIPTION

According to the Technical Regulations for Electrical and Telecommunication Products and Components in Korea, the DC supply voltage is specified to be less than 60 V in the charging system of small electric vehicles such as electric scooters. Therefore, in order to charge E-mobility equipment with a range of voltages, there is a need for charging systems capable of generating voltage more than 60 V.

Figure 2 shows the topology of the proposed multi-level E-mobility charging system. As shown in the figure, the structure of the charging system consists of independent buck converters connected in series, and the output voltage of each converter is overlapped. In general, multi-level topologies are used to cope with high voltage converters by overcoming the voltage limit of switching elements. However, the multi-level charging system for charging PMDs has a characteristic that each level input voltage of the converter uses a voltage capable of driving a general gate amplifier. Therefore, in this study, by using gate amplifier voltage as the power supply voltage through the configuration of the field-effect transistor (FET), a switch of the buck converter in the negative terminal of the input power supply. As a result, the system was easily built without the power supply of a separate independent gate amplifier and reducing the unit cost of charging system [16]–[18].

The output voltage of the multi-level converter proposed in this paper can be controlled by the state and duty ratio of the switch configured in the system. The input power of each level in the multi-level converter is represented by V_{iML}, and the sum of the voltage according to the switching state of the multi-level converter is represented by V_{ML} [19], [20].

In the case of the multi-level converter proposed in this study, a single buck converter is connected in series. Therefore, we first investigated the characteristics of the buck converter. For a typical buck converter, the inductor current ripple is determined by the specified voltage, frequency, and duty ratio [21]. Figure 3 shows the current ripple flowing through the inductor and the voltage ripple of the output voltage. If the current flowing through the inductor (L) is defined as i_L, the current ripple Δi_L of the inductor is expressed as Equation (1). In addition, if the output voltage is defined as V_0 and the output voltage ripple is defined as Δv_o, it can be expressed as Equation (2) [22]–[25].

$$\Delta i_L = \frac{T_s}{L} \times V_i d\,(1-d) \tag{1}$$

$$\Delta v_o = \frac{V_i d(1-d) \times T_s^2}{8LC} \tag{2}$$

For a typical buck converter, V_i, T_s, L, and C are determined by design conditions as seen in Equations (1) and (2) [26]–[29]. When controlling the converter, the current and output voltage ripple of the inductor are determined only by the duty ratio, and the ripple is maximized when the duty ratio is 0.5. However, for the case of the multi-level buck converter proposed in this paper, the current and voltage ripple of the inductor are determined by the number of levels and duty ratio of the converter, and the condition in which the ripple is maximized equals the number of levels of the converter. This is explained in detail as follows. Compared to the input voltage V_i of a conventional buck converter, the input of the multi-level converter consisting of N_{total} becomes V_i/N_{total}; in this study, we defined it as V_{iML}. The number of levels

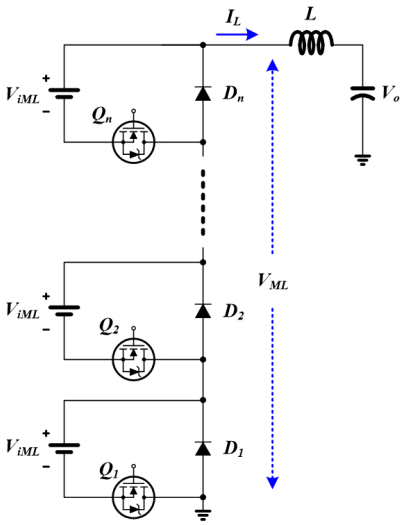

FIGURE 2. Topology of the proposed multi-level charging system.

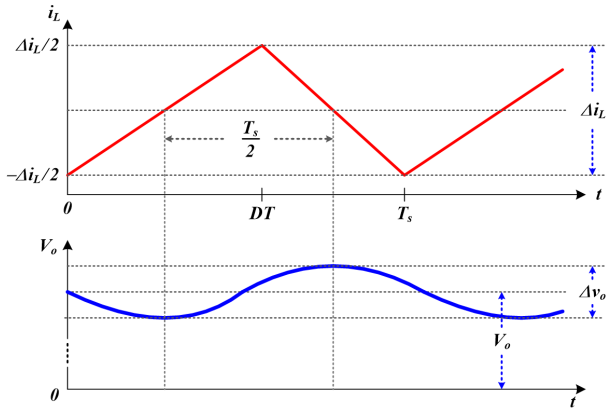

FIGURE 3. Current and voltage ripple of a typical buck converter.

N_{ML} of the multi-level converter that operates by using V_{iML} as an input in order to generate the output voltage V_o is determined, and the number of converters performing pulse-width modulation (PWM) between 0 < duty < 1 is defined as N_{MLd}. If the switching state of the converter is duty = 1, it is excluded from the number of converters N_{MLd} performing PWM, and through this definition, the duty ratio d_{ML} of the output voltages V_o and N_{MLd} can be expressed as

$$V_o = V_{iML} \times (N_{ML} + (d_{ML} - 1)\, N_{MLd}) \tag{3}$$

$$d_{ML} = \frac{V_o - (V_{iML} \times (N_{ML} - N_{MLd}))}{V_{iML} \times N_{MLd}} \tag{4}$$

If the number of converters N_{MLd} switching between $0 < d_{ML} < 1$ is 1, the current ripple and output voltage ripple of the inductor can be expressed as

$$\Delta i_L = \frac{T_s}{L} \times V_{iML} d_{ML}(1 - d_{ML}) \tag{5}$$

$$\Delta v_o = \frac{V_{iML} d_{ML}(1 - d_{ML}) \times T_s^2}{8LC} \tag{6}$$

However, if $N_{MLd} > 1$, then the current is interleaved by N_{MLd}, resulting in reducing the current ripple Δi_L flowing through the inductor as much as the current ripple cancellation effect k_{irce}. The current ripple cancellation effect k_{irce} can be expressed as

$$k_{irce} = \frac{N_{MLd} \times \left(d_{ML} - \frac{m}{N_{MLd}}\right) \times \left(\frac{m+1}{N_{MLd}} - d_{ML}\right)}{d_{ML} \times (1 - d_{ML})} \tag{7}$$

Here, $m = N_{MLd} \times d_{ML}$ is the largest integer that does not exceed $N_{ML} \times d_{ML}$.

The current ripple and output voltage ripple of the inductor, reduced as much as the current ripple cancellation effect k_{irce}, can be expressed as Equations (8) and (9), respectively.

$$\Delta i_L = \frac{k_{irce} T_s}{L} \times V_{iML} d_{ML}(1 - d_{ML}) \tag{8}$$

$$\Delta v_o = \frac{V_{iML} d_{ML}(1 - d_{ML}) \times T_s^2}{8LC \times N_{MLd}} \tag{9}$$

As expressed in Equations (5) and (6), the input voltage is reduced by the number of multi-level converters N_{total}, compared to the conventional buck converter, thus confirming that the inductor current ripple can be reduced. In addition, depending on the switching operation method of the multi-level converter, the current ripple and output voltage ripple of the inductor can be further reduced as confirmed in Equations (8) and (9). Even for the region where the duty ratio is 0.5, at which the output voltage ripple is largest, Equations (6) and (9) confirm that the output voltage ripple is much smaller than that of the conventional single buck converter.

Figures 4 and 5 show the normalized size of the input ripple current and output ripple current reduction depending on the number and duty ratio of the converters that make up the charging system when $N_{MLd} = 1$. As confirmed in the figures, the inductor ripple current is eliminated as the number of levels increases in the multi-level charging system, resulting in a smaller ripple current flowing into the output

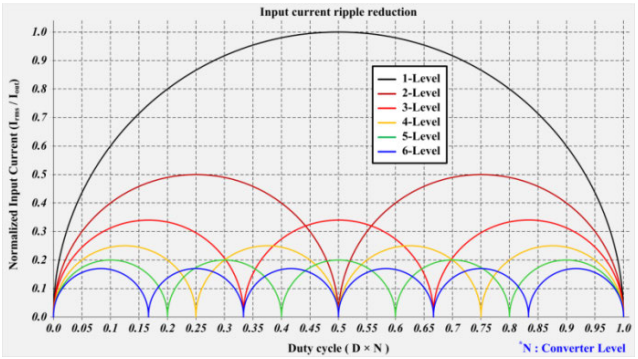

FIGURE 4. Normalized RMS input ripple current vs. duty circle.

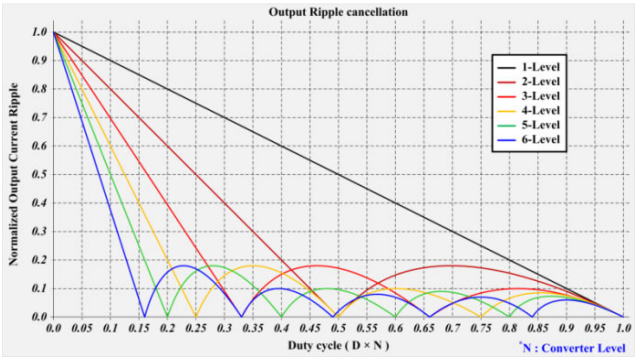

FIGURE 5. Normalized output current ripple vs. duty circle.

filter capacitor. When N_{MLd} increases as the number of levels N_{ML} in the multi-level charging system increases, the inductor current ripple size can be further reduced. Consequently, because increasing the number of levels N_{ML} of the multi-level converter and N_{MLd} is the same as the effect of increasing the frequency, the inductor value and capacitor value of the L-C filter present on the output can be reduced, resulting in device size reduction. It also means that a very wide region of the output voltage can be controlled and the current ripple rate required by various batteries can be satisfied.

B. OPTIMAL OPERATION METHOD OF MULTI-LEVEL CONVERTERS

As mentioned previously, because increasing the number of levels N_{ML} of the multi-level converter and N_{MLd} has the same effect as increasing the frequency, the current ripple rate can be greatly reduced, resulting in satisfying the current ripple rate required by various batteries. However, if we let N_{MLd} be equal to N_{ML} in order to reduce the ripple of the multi-level converter, the system efficiency is reduced by the switching loss. Therefore, an operation method is needed that can satisfy the current ripple rate required by a specific battery while optimizing efficiency by minimizing N_{MLd}. Figure 6 shows a flowchart for the optimal operation of the multi-level converter.

The flowchart in Figure 6 can be divided into two main phases. N_{ML} and N_{MLd} are determined first to satisfy the battery charge ripple requirement Δi_{Brqr} in all regions regardless

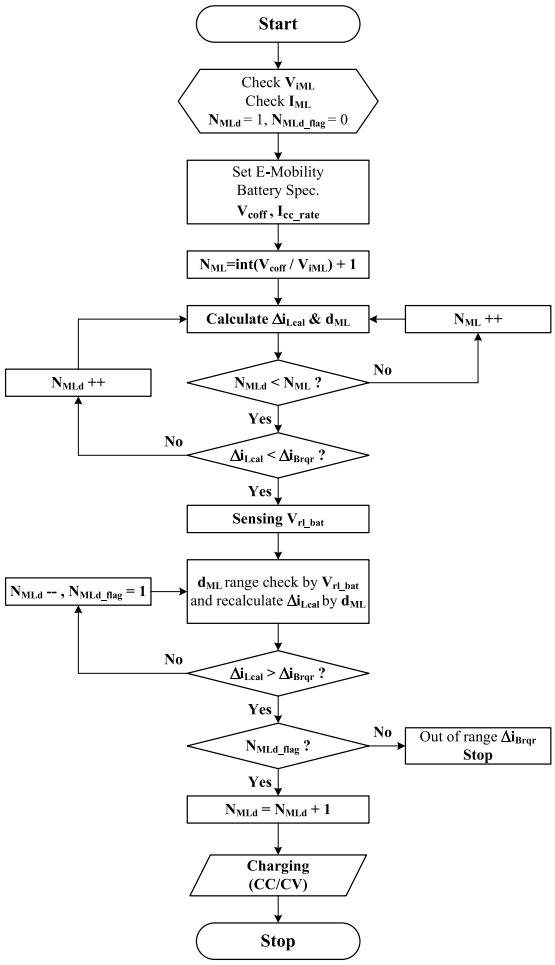

V_{iML} [V] : Input voltage for each level of multi-level converter
I_{ML} [A] : Output rated current of multi-level converter
N_{ML} : Number of multi-level converters driven
N_{MLd} : Number of multi-level converters operating in duty ($0 < d_{ML} < 1$)
N_{MLd_flag} : Number of multi-level converters operating flag
V_{coff} [V] : Cut off voltage of battery
V_{rl_bat} [V] : Real voltage of battery
I_{cc_rate} [A] : Rated current of battery
ΔI_{Lcal} [A] : Calculated current ripple current of multi-level converter
ΔI_{Brqr} [A] : Required ripple rate of battery

FIGURE 6. Flowchart of the optimal operation of the multi-level converter.

of the current voltage state of a battery. After determining N_{ML} and N_{MLd}, the optimal operation is performed to minimize switching loss by determining a minimum value of N_{MLd} that satisfies the charge ripple requirement Δi_{Brqr} of the battery through the actual voltage sensing of the battery.

Figure 7 shows a schematic diagram of the switching operation state of the charging system driving for optimal operation on the basis of the flowchart. Three levels were assumed for the sake of convenience.

When the multi-level converter is composed of three levels as shown in Figure 7, the current ripple size changes according to the switching state. Here, two conditions satisfy the current ripple rate required by a specific battery, and the state at this time is when $N_{MLd} > 1$. As described previously, because a relatively high efficiency condition can be achieved

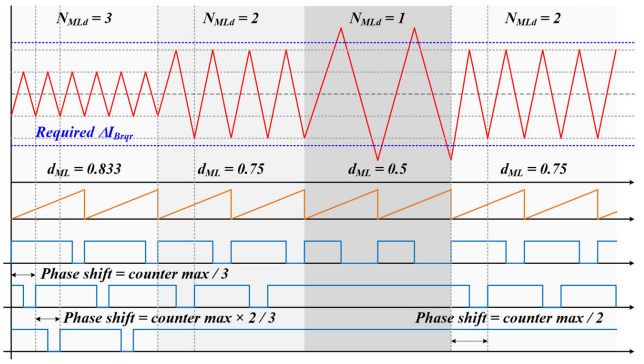

FIGURE 7. Operation for the optimal operation of the multi-level converter.

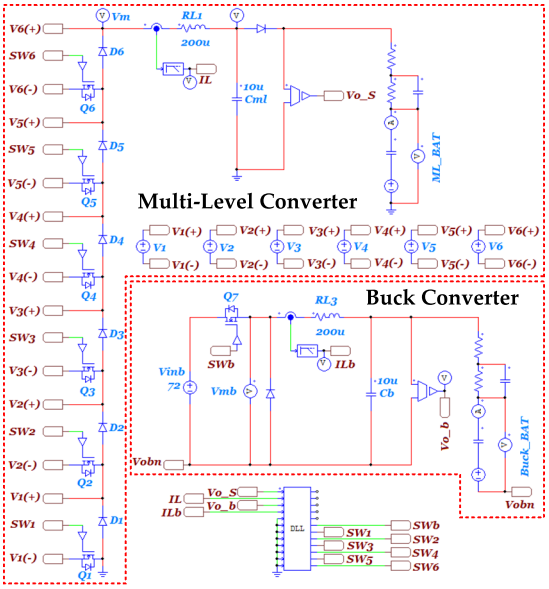

FIGURE 8. Simulation circuit diagram.

when $N_{MLd} = 2$ while also satisfying the current ripple rate of the battery, it is desirable to operate two converters for switching.

IV. MULTI-LEVEL CHARGING SYSTEM FOR PMDs

A. SIMULATION

Figure 8 shows the simulation circuit diagram used to verify the validity of the proposed multi-level charging system. The simulation circuit diagram is composed mainly of a conventional buck converter and the multi-level converter proposed in this paper. First, we controlled the voltage to increase it linearly from 0 V to 70 V in order to check the inductor current ripple and the output voltage ripple according to each voltage region. Here, in order to clearly compare the size of the current flowing through the inductor, we designed the inductance value of the inductor as the minimum value at which continuous current can flow. In order to compare the output voltage ripple, we performed simulations by designing the capacitance value of the condenser in a way that the output voltage ripple was less than 5%.

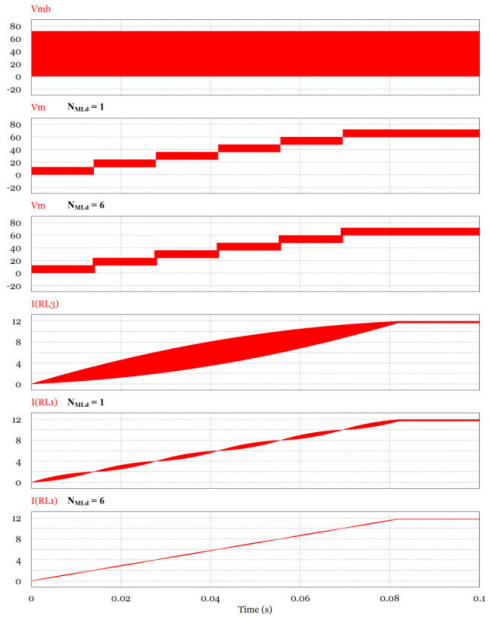

FIGURE 9. Converter operation characteristic waveforms.

TABLE 2. Specifications and parameters of the simulation circuit.

Note	Symbol	Value
Buck converter input voltage	Vinb	72 V
Multi-level converter input voltage	V1 ~ V6	12 V
Output inductor inductance	RL1, RL3	200 µH
Output capacitor capacitance	Cml, Cb	10 µF
Output load resistance	Rload	6 Ω
Switching frequency	fs	20 kHz

Figure 9 shows the voltage and inductor current waveform by PWM of the conventional buck converter and the proposed multi-level converter. Here, the simulation results of the multi-level converter were compared using the number of converters that operate switching when $N_{MLd} = 1$ and $N_{ML} = N_{MLd}$. Table 2 shows the parameter specification of the simulation circuit.

As confirmed in the waveforms of the simulation results, it can be verified that the voltage and output current ripple by PWM of the multi-level charging system proposed in this paper decrease significantly compared to the conventional single buck converter. The current ripple decreases further as N_{MLd} increases.

Figure 10 shows the waveform of the battery charging simulation results for a charging system consisting of a conventional buck converter and the multi-level converter. The battery in the simulations was configured with a Randles model represented by an electrical equivalent circuit. Here, we conducted the simulations without accounting for the parasitic inductance caused by contacting the battery terminals at high frequency. In order to shorten the simulation time, it was assumed that the initial charging voltage of the battery was 56 V, and the system was operated in CC-CV mode

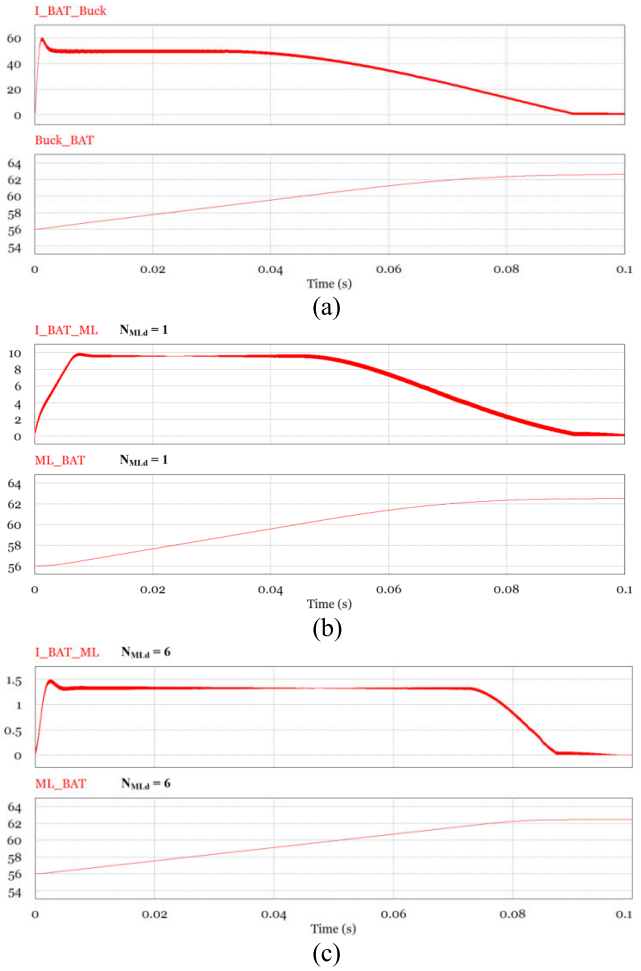

FIGURE 10. Battery charging simulation results: (a) Buck converter, (b) multi-Level converter for $N_{MLd} = 1$, and (c) multi-Level converter for $N_{MLd} = 6$.

by configuring the battery equivalent model with an end-of-charge voltage of 62 V. To satisfy the charging current ripple rate of batteries with various capacities, the current ripple rate must be satisfied even in a low-current region. Therefore, we conducted the simulations to verify the minimum current that can satisfy the charging current ripple rate of 5% or less for each system on the basis of the parameters shown in Table 2.

Figure 10(a) shows the battery charging simulation results of the single buck converter. The battery minimum charging current is 50 A, and at this time the current ripple Δi_L is approximately 2.15 A for a current ripple rate of approximately 4.3%. Figure 10(b) shows the battery charging simulation results of the multi-level converter under the condition of $N_{ML} = 6$ and $N_{MLd} = 1$. At this time, the battery minimum charging current is 10 A, the current ripple Δi_L is approximately 0.416 A, for a current ripple rate of approximately 4.16%. Figure 10(c) shows the battery charging simulation results of the multi-level converter when the condition is $N_{ML} = 6$ and $N_{MLd} = 6$. The battery minimum charging current is 1.5 A, and at this time the current

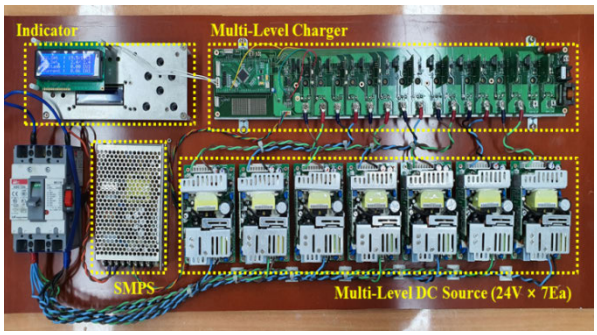

FIGURE 11. Multi-Level charger for the experiment.

ripple Δi_L is approximately 0.07 A, for a current ripple rate of approximately 4.6%.

Through the simulations, we confirmed that the current ripple is reduced in all regions compared to the current ripple of the conventional single buck converter when using multi-level converter hardware. We also confirmed that the current ripple decreased with increasing N_{MLd}. Therefore, we verified that the multi-level converter hardware and operation method proposed in this paper can satisfy the charging voltage and current ripple rate of a very wide range of batteries, and can be operated efficiently through algorithms that minimize switching loss during system operation.

B. EXPERIMENT

Figure 11 shows the charging system for verifying the operation of the multi-level converter. The configuration of the system consists of the multi-level converter with a total of seven levels and a multi-level power supply using 200-W SMPS (Switching Mode Power Supply) with seven 24-V outputs. Of them, only six levels are used to output up to 140 V. The one remaining level is reserved for use in case the multi-level buck converter fails.

We conducted experiments under two conditions in order to accurately compare the operating characteristics of the proposed multi-level converter. The parameters of the conditions are shown in Table 3.

First, in order to confirm the current ripple reduction characteristics by N_{ML} and N_{MLd} of the multi-level converter, we conducted experiments with the experimental condition 1 that could generate stable output voltage. The voltage was controlled to increase linearly from minimum output voltage (0 V) to maximum output voltage (140 V) by providing a fixed resistive load on the output of the charger. The analysis result waveforms were obtained by comparing

TABLE 3. Specifications and parameters of experiment.

Note	Condition 1	Condition 2
Output inductor's inductance	200 μH	200 μH
Output capacitor capacitance	220 μF	10 μF
Output load resistance	17.14 Ω	17.14 Ω
Switching frequency	20 kHz	5 kHz

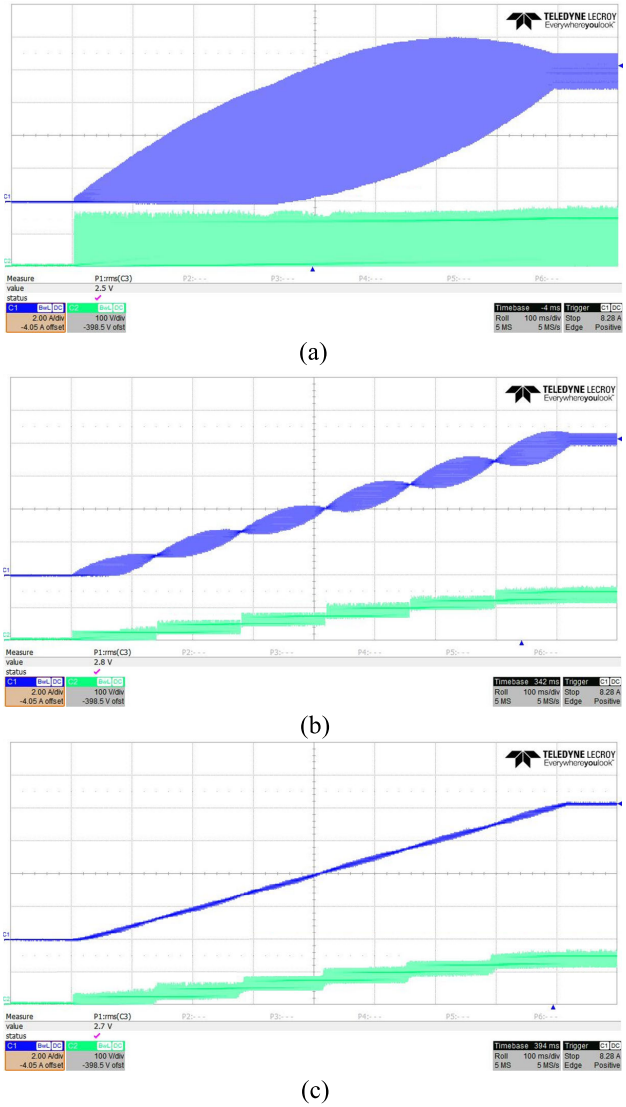

FIGURE 12. Voltage waveform by inductor current ripple and PWM: Ch1: 2 A/div, Ch2: 100 V/div, (a) Single buck converter, (b) multi-level converter for $N_{MLd} = 1$ and (c) multi-level converter for $N_{ML} = 6$.

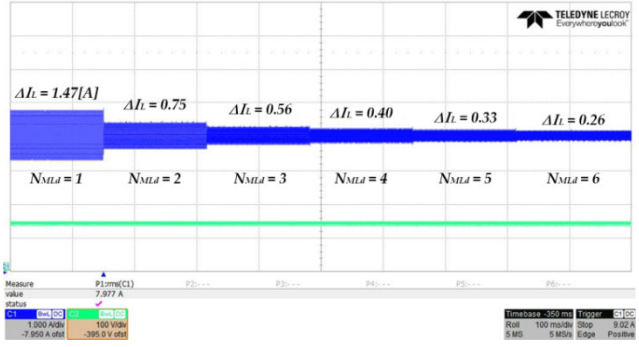

FIGURE 13. Current ripple characteristic waveform according to changes in N_{MLd}: Ch1: 1 A/div, Ch2: 100 V/div.

the characteristics through the inductor current ripple Δi_L (ch1: blue) according to the converter type and the voltage V_{ML}(ch2: green) by PWM, as shown in Figure 12.

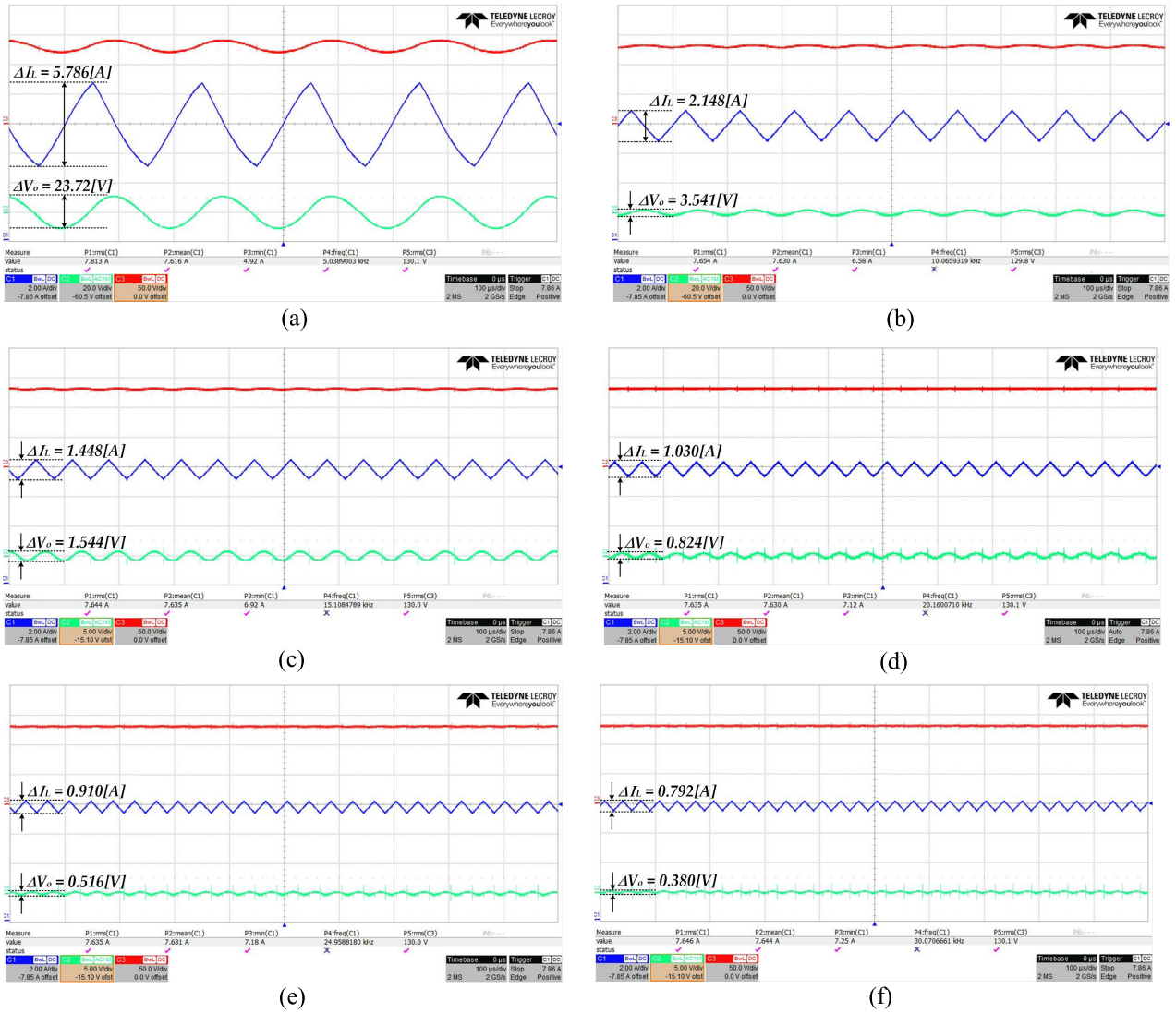

FIGURE 14. Current ripple, voltage ripple, and output voltage waveforms according to changes in N_{MLd}: (a) Ch1: 2 A/div, Ch2: 20 V/div, Ch3: 50 V/div; (b) Ch1: 2 A/div, Ch2: 20 V/div, Ch3: 50 V/div; (c) Ch1: 2 A/div, Ch2: 5 V/div, Ch3: 50 V/div; (d) Ch1: 2 A/div, Ch2: 5 V/div, Ch3: 50 V/div; (e) Ch1: 2 A/div, Ch2: 5 V/div, Ch3: 50 V/div; (f) Ch1: 2 A/div, Ch2: 5 V/div, Ch3: 50 V/div.

As shown in Figure 12, the current ripple of the multi-level converter is reduced in all regions compared to the single buck converter. In addition, as mentioned previously, we confirmed that for the condition where the inductor current ripple of the multi-level converter was maximized, N_{ML} levels of the converter were performing the operation, and there was an increase in N_{MLd}.

In this condition, the current ripple increases significantly. Here, we checked the current ripple characteristics by continuously changing N_{MLd} from 1 to 6 levels in order to verify the reduction in current according to N_{MLd}, as shown in Figure 13.

Next, we configured the system with the experimental condition 2 in order to accurately compare the current ripple and output voltage ripple of the inductor according to the change in N_{MLd}. We conducted experiments by setting the duty ratio to 0.5, where the inductor current ripple was maximized. Figure 14 shows the result waveforms: the inductor current waveform (ch1), output voltage ripple (ch2), and output voltage (ch3). For the output voltage ripple, we conducted the experiments by setting the AC coupling state to measure only the ripple component in the oscilloscope. As shown in Figure 14, we confirmed that the same effect as an increase in the switching frequency occurs as N_{MLd} increases, which reduces the output voltage ripple along with the current ripple. From the experimental data, we confirmed that the reduction in the current ripple and output voltage ripple were by factors of 7.3 and 62.4 for $N_{MLd} = 1$ and $N_{MLd} = 6$, respectively.

Figure 15 shows a measurement of the output efficiency, operating in constant current charging mode of 8.2 A. Formally, the input power of the 6-channel output 1 channel shall be measured to measure the efficiency of the multi-level converter. However, in the experiment, the AC input

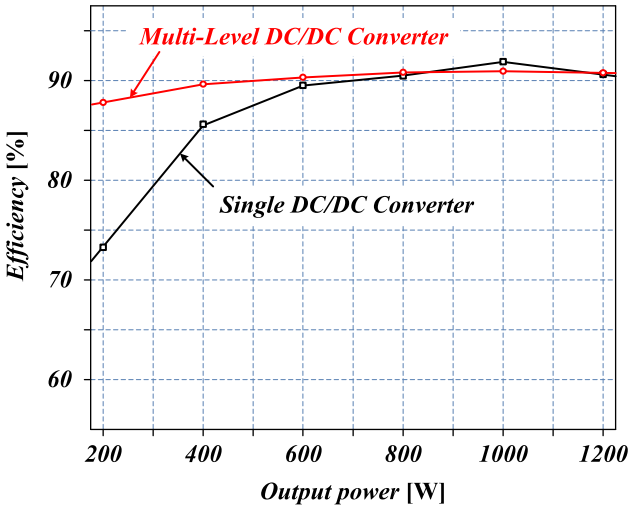

FIGURE 15. Efficiency curve, Multi-level and single buck converter.

power and DC output power were measured to confirm the system efficiency for abbreviation. In this case, the same input power was used in a 6-series configuration to compare the relative efficiency of a single converter rather than a multi-level converter. As shown in Figure 15, for existing single charging system, it can be seen that the battery has low-efficiency in light-load areas with low voltage and has high-efficiency in rated-load with high charging-voltage. However, in the case of multi-level converters, the maximum efficiency is lower than that of a single converter system, but the efficiency variation, due to the charging voltage, occurs less frequently in the range, from light-load to the rated-load. This is expected to be highly applicable to charging stations as it has the advantage of securing a constant current ripple and maintaining efficiency, regardless of the charging operation voltage of E-Mobility with various charging voltage.

V. CONCLUSION

This paper proposes the topology for a multi-level charging system capable of charging small electric vehicles. We verified the validity of the proposed multi-level charging system through simulations and experiments, and drew the following conclusions:

1. By developing a topology with a structure that shares power by subdividing the power supply, we propose a single charging system with a very wide range of charging voltage that can satisfy the charging requirements such as the current ripple and voltage ripple of various types of E-mobility equipment batteries, and an optimal switching technique to operate the system.

2. The same effect as raising the switching frequency can be obtained depending on the operation state and the number of multi-level converters using the subdivided power supply as input. Consequently, there is an advantage that the input ripple current is reduced, thus not only minimizing the input capacitor used to meet the safety certification standards but also easing the requirements of ESR (Equivalent Serial Resistance). In addition, the current ripple and output voltage ripple of the inductor are reduced, thus decreasing the value and size of the L-C filter present in the output stage, resulting in a reduction in the unit cost and size of the charging system.

3. Because the size of the input power decreases as the number of the multi-level converters increases, the voltage of the semiconductor devices including the switch devices configured in the converter can be set low, which reduces the unit cost and increases the availability of the parts needed to build the charging system

Therefore, the multi-level charging system proposed in this paper is expected to contribute to the commercialization and distribution of small electric vehicles by increasing the availability of charging options.

ACKNOWLEDGMENT

The authors would like to thank Editage (www.editage.co.kr) for English language skills.

REFERENCES

[1] M. M. Thackeray, C. Wolverton, and E. D. Isaacs, "Electrical energy storage for transportation—approaching the limits of, and going beyond, lithium-ion batteries," *Energy Environ. Sci.*, vol. 5, no. 7, p. 7854–7863, Apr. 2012.
[2] M. Momirlan and T. Veziroglu, "The properties of hydrogen as fuel tomorrow in sustainable energy system for a cleaner planet," *Int. J. Hydrogen Energy*, vol. 30, no. 7, pp. 795–802, Jul. 2005.
[3] T. R. Hawkins, B. Singh, G. Majeau-Bettez, and A. H. Strømman, "Comparative environmental life cycle assessment of conventional and electric vehicles," *J. Ind. Ecol.*, vol. 17, no. 1, pp. 53–64, Feb. 2013.
[4] J.-Y. Kuo, A. Sayeed, N. T. Tangirala, V. C. Y. Han, J. Dauwels, and M. P. Mayer, "Pedestrians' acceptance of personal mobility devices on the shared path: A structural equation modelling approach," in *Proc. IEEE Intell. Transp. Syst. Conf. (ITSC)*, Oct. 2019, pp. 2349–2354.
[5] S. Magasi, A. Wong, A. Miskovic, D. Tulsky, and A. W. Heinemann, "Mobility device quality affects participation outcomes for people with disabilities: A structural equation modeling analysis," *Arch. Phys. Med. Rehabil.*, vol. 99, no. 1, pp. 1–8, Jan. 2018.
[6] Y. Hasegawa, C. Dias, M. Iryo-Asano, and H. Nishiuchi, "Modeling pedestrians' subjective danger perception toward personal mobility vehicles," *Transp. Res. F, Traffic Psychol. Behav.*, vol. 56, pp. 256–267, Jul. 2018.
[7] F. Gebauer, R. Vilimek, A. Keinath, and C.-C. Carbon, "Changing attitudes towards e-mobility by actively elaborating fast-charging technology," *Technol. Forecasting Social Change*, vol. 106, pp. 31–36, May 2016.
[8] J. Schlund, R. Steinert, and M. Pruckner, "Coordinating E-Mobility charging for frequency containment reserve power provision," in *Proc. 9th Int. Conf. Future Energy Syst.-e-Energy*, Jun. 2018, pp. 556–563.
[9] S. Neujahr, M. Thummler, and A. Pretschner, "Modular platforms for E-mobility charging stations," in *Proc. 13th Int. Multi-Conf. Syst., Signals Devices (SSD)*, Mar. 2016, pp. 499–502.
[10] T. Haraguchi, I. Kageyama, and T. Kaneko, "Study of personal mobility vehicle (PMV) with active inward tilting mechanism on obstacle avoidance and energy efficiency," *Appl. Sci.*, vol. 9, no. 22, p. 4737, 2019.
[11] M. Tinnilä and J. Kallio, "Impact of future trends on personal mobility services," *Int. J. Automot. Technol. Manage.*, vol. 15, no. 4, pp. 401–417, 2015.
[12] N. Bergman, "Electric vehicles and the future of personal mobility in the United Kingdom," in *Transitions in Energy Efficiency and Demand: The Emergence, Diffusion and Impact of Low-Carbon Innovation*, K. E. H. Jenkins and D. Hopkins, Eds., 2019, pp. 53–71
[13] J. Barceló, "Future trends in sustainable transportation," in *Sustainable Transportation and Smart Logistics*. Amsterdam, The Netherlands: Elsevier, 2019, pp. 401–435.
[14] V. Nikulina, D. Simon, H. Ny, and H. Baumann, "Context-adapted urban planning for rapid transitioning of personal mobility towards sustainability: A systematic literature review," *Sustainability*, vol. 11, no. 4, p. 1007, 2019.

[15] H. Hayashi, T. Sasatani, Y. Narusue, and Y. Kawahara, "Design of wireless power transfer systems for personal mobility devices in city spaces," in *Proc. IEEE 90th Veh. Technol. Conf. (VTC-Fall)*, Sep. 2019, pp. 1–5.
[16] S. A. Nasirudeen *et al.*, "Summary of the key technologies for metric range extension of electric vehicles," *Arch. Current Res. Int.*, Vol. 18, no. 2, pp. 1–7, Aug. 2019.
[17] K. Suresh, N. Chellammal, C. Bharatiraja, P. Sanjeevikumar, F. Blaabjerg, and J. B. H. Nielsen, "Cost-efficient nonisolated three-port DC-DC converter for EV/HEV applications with energy storage," *Int. Trans. Elect. Energy Syst.*, vol. 29, no. 10, 2019, Art. no. e12088.
[18] C.-Y. Lim, Y. Jeong, and G.-W. Moon, "Phase-shifted full-bridge DC–DC converter with high efficiency and high power density using center-tapped clamp circuit for battery charging in electric vehicles," *IEEE Trans. Power Electron.*, vol. 34, no. 11, pp. 10945–10959, Nov. 2019.
[19] Y. Huangfu, L. Guo, R. Ma, and F. Gao, "An advanced robust noise suppression control of bidirectional DC-DC converter for fuel cell electric vehicle," *IEEE Trans. Transp. Electrific.*, vol. 5, no. 4, pp. 1268–1278, Dec. 2019.
[20] H. Moradisizkoohi, N. Elsayad, and O. A. Mohammed, "A family of three-port three-level converter based on asymmetrical bidirectional half-bridge topology for fuel cell electric vehicle applications," *IEEE Trans. Power Electron.*, vol. 34, no. 12, pp. 11706–11724, Dec. 2019.
[21] H. Tao, G. Zhang, and Z. Zheng, "Onboard charging DC/DC converter of electric vehicle based on synchronous rectification and characteristic analysis," *J. Adv. Transp.*, vol. 2019, pp. 1–10, Jun. 2019.
[22] M. Lee, C.-S. Yeh, O. Yu, J.-W. Kim, J.-M. Choe, and J.-S. Lai, "Modeling and control of three-level boost rectifier based medium-voltage solid-state transformer for DC fast charger application," *IEEE Trans. Transp. Electrific.*, vol. 5, no. 4, pp. 890–902, Dec. 2019.
[23] D. Chou, K. Fernandez, and R. C. N. Pilawa-Podgurski, "An interleaved 6-Level GaN bidirectional converter for level II electric vehicle charging," in *Proc. IEEE Appl. Power Electron. Conf. Expo. (APEC)*, Mar. 2019, pp. 594–600.
[24] S. Arof, N. H. N. Diyanah, P. Mawby, H. Arof, and N. M. Yaakop, "Low harmonics plug-in home charging electric vehicle battery charger utilizing multi-level rectifier, zero crossing and buck chopper," in *Progress in Engineering Technology*. Cham, Switzerland: Springer, 2019, pp. 103–118.
[25] W. Li, Z. Lin, H. Zhou, and G. Yan, "Multi-objective optimization for Cyber-Physical-Social systems: A case study of electric vehicles charging and discharging," *IEEE Access*, vol. 7, pp. 76754–76767, 2019.
[26] Fischer, Marcel, and Patrick Lattmann, "Ripple current reduction for wireless electric vehicle charging," U.S. Patent Appl. 15 709 314, Mar. 21, 2019.
[27] F. Yan, J. Li, C. Du, C. Zhao, W. Zhang, and Y. Zhang, "A coupled-inductor DC-DC converter with input current ripple minimization for fuel cell vehicles," *Energies*, vol. 12, no. 9, p. 1689, 2019.
[28] M.-K. Nguyen and Y.-O. Choi, "Voltage multiplier cell-based quasi-switched boost inverter with low input current ripple," *Electronics*, vol. 8, no. 2, p. 227, 2019.
[29] A. M. Prozorov, D. A. Nikitin, and A. D. Tarasov, "Techniques for reducing output current ripple in a flyback converter with PFC," in *Proc. Ural Symp. Biomed. Eng., Radioelectron. Inf. Technol. (USBEREIT)*, Apr. 2019, pp. 391–393.

SANG-KIL LIM (Member, IEEE) received the B.S. degree in mechanical engineering from Jeonbuk National University, in 2008, and the M.S. and Ph.D. degrees in electrical engineering from Chonnam National University, Gwangju, South Korea, in 2010 and 2017, respectively. Since 2019, he is holding a postdoctoral position at EV Components and Materials R&D Group, Korea Institute of Industrial Technology. Since 2020, he has been a Professor with the Department of Automotive Engineering, Honam University. His research interests include power electronics, power conditioning system dc–dc converters for renewable energy, and power conversion system for EVs.

HAE-SOL LEE (Student Member, IEEE) received the B.S. degree in mechanical engineering from Konkuk University, Seoul, South Korea, in 2017. He is currently pursuing the M.S. degree in robotics with the University of Science and Technology, Daejeon, South Korea. He is currently working as a Researcher with the EV Components and Materials R&D Group, Korea Institute of Industrial Technology. His research interests include hybrid electric vehicles (HEVs)/electric vehicles (EVs) motor drive systems and drive motor in unmanned aerial vehicles (UAVs).

HYUN-ROK CHA received the Ph.D. degree in physics from the Tokyo Institute of Technology, Tokyo, Japan, in 2009. He was with the Samsung Electronics Research Center, Gwangju, for a period of four years. Since 2004, he has been a Senior Researcher with the EV Components and Materials R&D Group, Korea Institute of Industrial Technology. His research interests include E-mobility, electric vehicle (EV) platforms, smart vehicle control hybrid-powered drone, and power electronics.

SUNG-JUN PARK (Member, IEEE) received the B.S., M.S., and Ph.D. degrees in electrical engineering, and the Ph.D. degree in mechanical engineering from Pusan National University, Busan, South Korea, in 1991, 1993, 1996, and 2002, respectively. From 1996 to 2000, he was an Assistant Professor with the Department of Electrical Engineering, Koje College, Geoje, South Korea. From 2000 to 2003, he was an Assistant Professor with the Department of Electrical Engineering, Tongmyong College, Busan. Since 2003, he has been a Professor with the Department of Electrical Engineering, Chonnam National University, Gwangju, South Korea. His research interests include power electronics, motor control, mechatronics, and micromachine automation.